On the pseudogap phase in high-T_c superconductors

P. Devillard[(a)] and J. Ranninger[(b)]

[(a)] *Centre de physique théorique de Marseille, C.P.T. Case 907,*
Centre National de la Recherche Scientifique, Luminy, 13288 Marseille Cédex 9, France
[(b)] *Centre de Recherches sur les Très Basses Températures, Laboratoire Associé à l'Université Joseph Fourier,*
Centre National de la Recherche Scientifique, BP 166, 38042, Grenoble Cédex 9, France

(February 1, 2008)

We describe the approach of the superconducting state as a sequence of cross-over phenomena. As the temperature is decreased, uncorrelated pairing of the electrons leads to the opening of a pseudogap at T_F^*. Upon further lowering the temperature those electron pairs acquire well behaved itinerant features at T_B^*, leading to partial Meissner screening and Drude type behavior of the optical conductivity. Further decrease of the temperature leads to their condensation and superconductivity at T_c. The analysis is done on the basis of the Boson-Fermion model in the cross-over regime between 2D and 3D.

PACS numbers: 74.72.-h, 74.25.Dw, 74.25.Gz, 74.25.-q

It is now generally accepted that the onset of superconductivity in high temperature superconductors (HTS) is controlled by phase fluctuations [1], whilst a finite amplitude of the order parameter is expected to persist up to some T^*, which can be well above T_c. It has also been argued [2] that the shrinking of the pseudogap phase (the interval $[T_c, T^*]$) with increased doping should be related to an increase of the superfluid density n_s rather than of the coherence length. In that case, doping of HTS should not induce a cross-over between a Bose-Einstein condensation (BEC) of preformed pairs and a BCS state and hence the opening of the pseudogap should be unrelated to the onset of superconducting fluctuations. These expectations seem to be confirmed by specific heat data [3], transient Meissner screening [4] and Andreev spectroscopy [5]. The picture evolves according to which a pseudogap opens up, exclusively driven by amplitude fluctuations (dynamical pair-formation, uncorrelated in space and not necessarily related to incipient superconductivity). At some lower temperature short-range and short-time correlations of the electron pairs set in, eventually driving the system into a superconducting state.

From a theoretical point of view these are questions which can be addressed without having to resort to a specific microscopic mechanism for electron pairing and can be studied on such models as the generalized BCS hamiltonian, the negative U Hubbard model or the Boson-Fermion model (BFM). These phenomenological models [6] which explicitly incorporate pair correlations, capture a number of normal state properties of the HTS.

In a classical BCS type superconductor long range phase coherence occurs as soon as short range amplitude correlations (in form of electron pairing) set in. A simple mean field treatment can perfectly describe this situation. On the contrary, in HTS amplitude and phase correlations are separated and a minimal treatment must contain the possibility of allowing for propagating modes of electron-pairs on a time scale of the order of the inverse zero temperature gap [7]. We shall here explore the intricate relations between the onset of pairing of the electrons, their becoming itinerant and ultimately their condensation. In order to separate these various features in approaching the superconducting state we study them in view of a dimensional cross-over such as to capture part of the doping induced changes when going from the under into the overdoped regime. The dimensional cross-over will be controlled by the degree of anisotropy of the electron dispersion. The anisotropy in the electric transport coefficients [8] lends itself to such a picture.

This study is based on the BFM, a phenomenological model which is particularly suited for that purpose. The notion of rather long lived short range pair correlations is introduced explicitly into this model by assuming the presence of localized tightly bound electron pairs which hybridize with pairs of itinerant electrons. We assume a system described by effective sites each of which can alternatively be occupied by either a bound electron-pair or a pair of itinerant electrons, uncorrelated with each other. For the present study we shall assume a homogeneous distribution of both the bound electron-pairs and the itinerant electrons. It is however feasible that the distribution between those constituents occurs in form of a phase-separated phase with dynamically fluctuating regions of predominantly bound electron-pairs and regions with predominantly electrons, leading to "stripe phases". Previous studies of the BFM [9], based on conserving diagrammatic approximations let one envisage a well defined finite temperature interval for the pseudogap phase in 1D and 2D, while for 3D such a phase [10] should be restricted to a very narrow temperature regime above T_c. This suggests that the nature of the pseudogap phase should depend on dimensionality and that the pair-fluctuations which control it have, depending on temperature, different characteristics as far as superconducting fluctuations are concerned. We expect that at least two energy scales should be involved here, identifiable as two

temperatures: $T_F^* \equiv T^*$ and $T_B^* \leq T_F^*$,

- T_F^* corresponding to the opening of the pseudogap in the DOS of the electrons due to the onset of strong local correlations leading to electron pairing, uncorrelated in space.

- T_B^* corresponding to those local pair states becoming well defined itinerant excitations due to the onset of temporal and spatial correlations.

We shall determine the dependence of T_F^* and T_B^* on dimensionality by monitoring the anisotropy of the ratio of the electron mass orthogonal to the basal plane to that within it, $\alpha = m_\perp/m_\parallel$ in the bare electron dispersion

$$\varepsilon_{\mathbf{k}} = \frac{1}{m_\parallel}\left(\frac{|\mathbf{k}_\parallel|}{\pi}\right)^2 + \frac{1}{m_\perp}\left(\frac{|\mathbf{k}_\perp|}{\pi}\right)^2 - \mu$$

The BFM is then defined by the following Hamiltonian

$$H = \sum_{\mathbf{k},\sigma} \varepsilon_{\mathbf{k}} c_{\mathbf{k}\sigma}^\dagger c_{\mathbf{k}\sigma} + E_0 \sum_{\mathbf{q}} b_{\mathbf{q}}^\dagger b_{\mathbf{q}} + v \sum_{\mathbf{k}}[b_{\mathbf{q}}^\dagger c_{\mathbf{k}+\mathbf{q}\downarrow} c_{-\mathbf{k}\uparrow} + h.c.],$$

with $E_0 = \Delta_B - 2\mu$ and v denoting the pair-exchange coupling constant. $c_{\mathbf{k}\sigma}^{(\dagger)}$ denote fermionic operators for electrons with spin σ and wavevector $\mathbf{k}$ and $b_{\mathbf{q}}^{(\dagger)}$ describe tightly bound electron pairs which will be considered as simple Bosons. The chemical potential μ is common to Fermions and Bosons (up to a factor 2 for the Bosons) in order to guarantee charge conservation. We examine this model within the lowest order self-consistent conserving diagrammatic approximation for which the self-energies for the Fermions and Bosons are given by:

$$Im\Sigma_B(\mathbf{q},\omega) = -\frac{v^2}{2\pi}\int\frac{d^3k}{(2\pi)^3}\int d\varepsilon\, ImG_F(\mathbf{k}-\mathbf{q},\omega-\varepsilon)$$

$$ImG_F(\mathbf{k},\varepsilon)\left(tanh(\frac{\varepsilon}{2k_BT}) - tanh(\frac{\varepsilon-\omega}{2k_BT})\right)$$

$$Im\Sigma_F(\mathbf{k},\omega) = \frac{v^2}{2\pi}\int\frac{d^3q}{(2\pi)^3}\int d\varepsilon\, ImG_F(\mathbf{k}-\mathbf{q},\varepsilon-\omega)$$

$$ImG_B(\mathbf{q},\varepsilon)\left(tanh(\frac{\varepsilon-\omega}{2k_BT}) - cotanh(\frac{\varepsilon}{2k_BT})\right).$$

$G_F(\mathbf{k},\omega) = [\omega - \varepsilon_{\mathbf{k}} - Re\Sigma_F(\mathbf{k},\omega) - iIm\Sigma_F(\mathbf{k},\omega)]^{-1}$ and $G_B(\mathbf{q},\varepsilon) = [\omega - E_0 - Re\Sigma_B(\mathbf{q},\omega) - iIm\Sigma_B(\mathbf{q},\omega)]^{-1}$ denote the fully renormalized Fermion and Boson Green's functions which have to be determined selfconsistently. The above set of equations for the Green's functions is solved by a standard iterative procedure. The integration over the momenta $\mathbf{k}_\parallel$ is carried out by summing over a grid of 1025 points in the interval $[0,\pi]$. The integration over frequencies is carried out slightly above the real axis i.e., taking $\omega = Re\,\omega + i\eta$ with $\eta = 0.01$ and by summation over 2048 real frequencies in the interval $[-2,2]$. Throughout the present work all energies are given in units of the bare basal plane bandwidth $\widetilde{D} = 8t_\parallel$.

The pseudogap features which result from the solution of the above set of equations depend strongly on dimensionality. In 1D and 2D the Fermionic self-energy is essentially determined by the term proportional to $cotanh$ which leads to the most divergent contribution. For 3D the major contribution to the self-energy comes from the term proportional to $tanh$ and does not give rise to a noticeable pseudogap effect. A pseudogap is only seen as we lower the temperature and approach T_c where the term proportional to $cotanh$ again becomes important.

The various parameters entering our Hamiltonian are determined such as to reproduce certain robust features of HTS. Pinning down the number of Bosons $n_B = \langle b_i^+ b_i\rangle$ in this model is not free of ambiguities, given our poor understanding of the doping process in these materials. For a system such as, for instance, YBCO the number of doping induced bound elelctron-pairs could possibly be given by half the number of dopant ions $O_2^{2-}(1)$ in the chains, thus varying between 0 and 0.5 per effective site. The number of fermions $n_F = \sum_\sigma \langle c_{i\sigma}^+ c_{i\sigma}\rangle$ is taken to be equal to 1 if the boson-fermion exchange coupling were absent. We thus obtain a total number of charge carriers $n_{tot} = n_F + 2n_B$ which should be contained between 1 and 2. As a representative example we choose $n_{tot} = 1.25$. In order to have $n_F \leq 1$ we fix the bosonic level as $\Delta_B = 1.1$. In order to obtain values for T^* of the order of a few hundred degrees K we choose $v = 0.1$.

The pseudogap manifests itself as a dip which emerges in the DOS of the electrons close to the chemical potential below a certain temperature T_F^*. Tracing the value of the DOS at this energy as a function of temperature permits to identify this characteristic temperature. The appearence of this pseudogap is linked, as we have discussed previously [9], to a breakdown of well defined single-electron excitations close to the Fermi surface. Concomitantly with this trend, two-electron states (local electron-pair resonances) emerge and upon lowering the temperature, acquire itinerant behaviour below a second characteristic temperature T_B^*. T_B^* is defined by the condition (see Fig.1) that the imaginary part divided by the real part of the Boson self-energy is small, i.e., $\gamma_q^B(T)/\omega_q^B(T) \equiv \Gamma_B(q_\parallel,\omega_B(q_\parallel,T),T)/\omega_B(q_\parallel,T) \leq 0.1$ for small q vectors such as $q_\parallel = 0.1$. Below T_B^* we find $\omega_B(q_\parallel) = \hbar^2 q_\parallel^2/2m_B(T)$ for $q \leq 0.2$ where $m_B(T)$ denotes the temperature dependent mass of the itinerant two-particle excitations.

The two-electron states, becoming well defined as the temperature decreases, goes hand in hand with a significant increase of the distribution function for those states with small wave vectors. It is this feature which leads to a finite value of the amplitude of the order parameter in the normal state whilst at the same time phase coherence is totally absent. The temperature T_c at which superconductivity sets in is determined by the condition that the two-electron excitations condense in a macroscopic quan-

tum state. According to the Hugenholtz-Pines theorem, it is determined by $\Delta_B - 2\mu - Re\Sigma_B(0,0) = 0$. We plot in Fig.1 these three characteristic temperatures as a function of α. Notice the opposite trends of T_F^* and T_c, approaching each other as the isotropic limit is approached, ($\alpha = 10$). This is reminiscent of the experimental situation in cuprate HTS materials, as we go from the underdoped towards the optimally doped regime and might hence partly be related to such a dimensional cross-over.
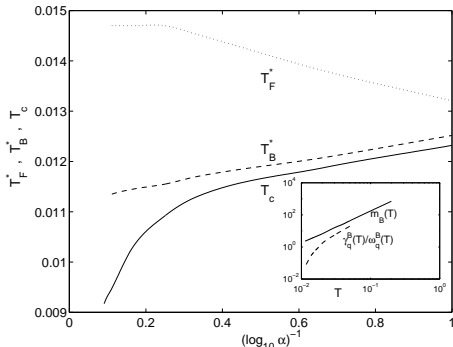

FIG. 1. Variation of T_F^*, T_B^* and T_c as a function of decreasing anisotropy. In the insert, the effective mass m_B (in units of $m_\parallel(T)$) of the itinerant in-plane bosonic excitations as a function of temperature (solid line) and the ratio of their width divided by their real part; for $\alpha = 10$.

In order to track such cross-over behavior in the pseudogap phase, leading from uncorrelated fluctuating electron pairs to their itinerant behavior as the temperature is decreased, we now show how such features are related to precursor Drude behavior of the optical conductivity and partial Meissner screening above T_c. We encounter here physics similar to that of the 2D non-interacting charged Bose gas [12], where a macroscopic number of itinerant bosonic states with momenta $\mathbf{k} \leq 1/\xi$ (ξ denoting the coherence length) act together collectively in a way similar to the macroscopically occupied condensed states with $\mathbf{k} = 0$ in the superconducting phase. The optical conductivity $\sigma(\mathbf{q}, \omega)$ and the diamagnetic susceptiblity $\chi(\mathbf{q}, \omega)$ are given by the longitudinal, respectively transverse part of the linear response to an external vector potential $\mathbf{A}(\mathbf{x}, t)$ depending on space and time. The resulting current is given by

$$\langle J_i(\mathbf{x}, t) \rangle = \frac{e^2}{m_\parallel^2 c} \int d^3 x dt K_{ij}(\mathbf{x} - \mathbf{x}', t - t') A_j(\mathbf{x}', t'),$$

$$K_{ij}(\mathbf{x}, t) = i\Theta(t)\langle [j_i(\mathbf{x}, t), j_j(0, 0)] \rangle - 2m_\parallel \delta(\mathbf{x})\delta(t)\delta_{ij} n^F(x)$$

where $n^F(x)$ denotes the density of the Fermions and $j_i^F(\mathbf{q}, t) = \sum_{\mathbf{k}} 2k_i c_{\mathbf{k}-\mathbf{q}/\mathbf{2}}^\dagger c_{\mathbf{k}+\mathbf{q}/\mathbf{2}}$ the Fourier transform of their current density. Putting

$$K_{ij}(\mathbf{q}, \omega) = \delta_{ij} i\omega \sigma(\mathbf{q}, \omega) - (q_i q_j - \delta_{ij} q^2)\chi(\mathbf{q}, \omega)$$

permits to extract the optical conductivity and diamagnetic susceptibility. The kernel $K_{ij}(\mathbf{x}, t)$ is decomposed

into two contributions. A first one is given by the simple bubble for the current autocorrelation function and neglecting vertex corrections. This is justified because of the strong incoherent contributions of G_F [9]. The second contribution to this kernel is evaluated in terms of the typical Aslamazov-Larkin diagram which takes into account the contributions of the itinerant Bosons. Due to the intrinsically localized nature of the Bosons there are no direct contributions of them to the electrical current. However since below T_B^* those bosonic two-electron excitations become itinerant they will, according to this Aslamazov-Larkin mechanism, contribute to substantially enhance the conductivity. This is manifest in the dc resistivity (see insert of Fig.2) which clearly shows that upon decreasing the anisotropy ratio α, the resistivity changes qualitatively from an upturn to a downturn as the temperature is lowered. Similarly, the effect of the pseudogap and the precursor to a macroscopic quantum state of the two-particle excitations can be tracked in the optical conductivity (Fig.2). By inspection of Fig. 2 we notice that for frequencies above $\simeq 0.01$ the optical conductivity drops as the temperature is decreased below $T = 0.03$ (indicative of a remnance of the pseudogap in the DOS of the single-electron states), while for frequencies below $\simeq 0.01$ the optical conductivity for those temperatures increases (indicative of an emerging precursor "Drude" component as we approach T_c). The crossover temperature at $T = \simeq 0.01$ is identified as the temperature T_B^* where the electron-pairs become itinerant. As the temperature is lowered, spectral weight is shifted downwards from the frequency regime $[0.01 \leq \omega \leq 0.04]$ thus enhancing this "Drude" component below 0.01. Such a redistribution of spectral weight is in fact observed [11]. For frequencies below 0.001 ($\simeq 240\,GHz$, taking $\widetilde{D} = 1\,eV$) the optical conductivity increases substantially as one approaches T_c.

Similarly, the real part of the diamagnetic susceptibility $\chi'(\mathbf{q}, \omega)$ for small wavevectors ($q \leq 1/\xi$, $\xi = 1/\sqrt{2m_B(T)\omega_0^B}$ denoting the coherence length) and frequencies is negative and small for high temperatures. It is given by the usual Landau diamagnetism of the electrons arising from the first contribution to the kernel K_{ij}. For temperatures below T_B^* (which is 0.01163 for a representative example of $\alpha = 10^3$) we calculate $\chi'(q, \omega)$, not taking into account the phase fluctuations. Close to T_c ($= 0.01127$ for $\alpha = 10^3$) $\chi'(q, 0)$ however is expected to diverge as $1/\xi_{KTB}^2$, where ξ_{KTB}^2 is the Kosterlitz-Thouless-Berezinskii coherence length for phase fluctuations. Our calculated $\chi'(q, \omega)$ increases significantly (roughly by a factor 50) over the Landau diamagnetism (see Fig. 3). It is given by the Aslamazov-Larkin contribution of K_{ij} i.e., $\chi'(0, 0) \simeq -av^4(\frac{e^2}{24\pi m_B(T)c^2}\frac{k_B T}{\omega_0^B})$, a being a numerical factor of order unity. The expression in the bracket corresponds to that known from the 2D

3

Bose gas [12]. It is this contribution which leads to almost complete Meissner screening. A characteristic frequency scale thus emerges below which phase uncorrelated amplitude fluctuations of the electron-pairs behave in some respects as condensed electron-pairs in the superconducting state. For frequencies $\omega \geq 10^{-5}$ we find the usual Landau diamagnetism but for $\omega \leq 10^{-5}$ we notice a saturation of $\chi'(\mathbf{q}, \omega)$ which decreases as the temperature increases. It is in this low frequency regime that we can extract from the diamagnetic susceptibility an almost complete Meissner screening for strong anisotropies. Its physical meaningfulness arises from the fact that for such a system there is phase locking over a given finite distance which is controlled essentially by the thermal wavelength of the itinerant Bosons [13].

optical conductivity showing Drude behavior.

FIG. 3. Real part of the in-plane diamagnetic susceptibility for small q and frequency $\omega = 0$ as a function of temperature. In the insert, its frequency dependence for different temperatures. $\alpha = 1000$.
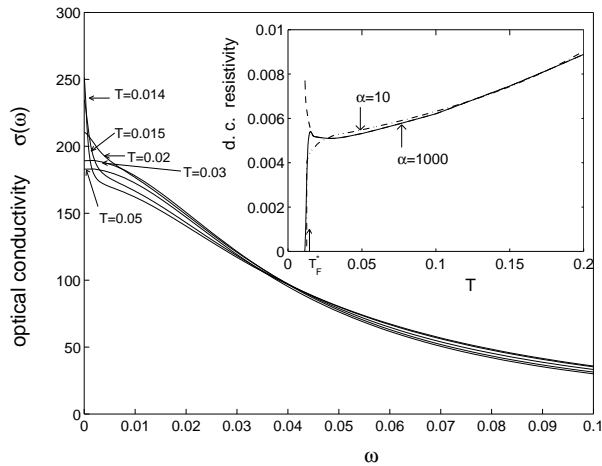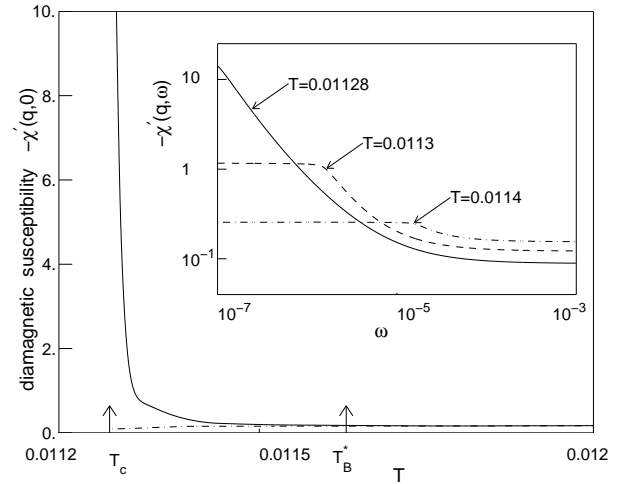
FIG. 2. The in-plane optical conductivity (arbitrary units) for a set of different temperatures and $\alpha = 10$. The inset illustrates the d.c. resistivity as a function of T, for $\alpha = 10$ including Aslamazov-Larkin contributions corrections (dashed dotted line) and for $\alpha = 1000$ including (solid line), respectively excluding them (dashed line). The arrow on the T axes indicates T_F^* for $\alpha = 1000$.

In this Letter we have examined the effect of pure amplitude fluctuations in the pseudogap phase of HTS as the dimensionality of the system varies between quasi-2D and quasi-3D. We conclude that the doping induced cross-over between the under- and the over-doped regime might at least partly be related to such a dimensional cross-over, clearly indicating a shrinking of the temperature regime for the pseudogap phase as the optimally doped limit is approached. We identified two characteristic temperatures in the pseudogap phase. The first one, T_F^*, corresponding to the opening of the pseudogap due to the onset of local uncorrelated electron-pair correlations. The second one, T_B^*, corresponding to the onset of itinerant behavior of those electron-pairs, below which we expect partial Meissner screening (very similar to that expected for the 2D non-interacting charged Bose gas, i.e., in the absence of any phase fluctuations) and an

[1] B. K. Chakraverty, A. Tharapder and M. Avignon, Physica C **235-240**, 2323 (1994): B. K. Chakraverty and T. V. Ramakrishnan, Physica C **282-287**, 290 (1997).
[2] V. Emery and S. Kivelson, Nature **374**, 434 (1995); ibid. J. Chem. Phys. Solids **59**, 1205 (1998).
[3] see for instance J. Loram et al., J. Phys. Chem. Solids **59**, 2091 (1998).
[4] J. Corson et al., Nature **398**, 221 (1999).
[5] G. Deutscher, Nature **397**,410 (1999).
[6] M. Randeria, Proc. Int. School of Physics "Enrico Fermi", Course CXXXVI, eds. G. Iadonisi, R. Schrieffer and M. L. Chiofalo (IOS Press, Amsterdam, 1998) p. 53; J. Ranninger and J. -M. Robin, ibid p 425.
[7] O. Tchernishyov, Phys. Rev. B **56**, 3372 (1997).
[8] K. Takenaka, K. Mizuhashi, H. Takagi and S. Uchida, Phys. Rev. B **50**, 6534 (1994); S. L. Cooper and K. E. Gray in "Physical Properties of high temperature superconductors", ed. D. M. Ginsberg (World Scientific, 1994).
[9] J. Ranninger, J. -M. Robin and M. Eschrig, Phys. Rev. Lett. **74**, 4027 (1995); J. Ranninger and J. -M. Robin, Solid State Commun. **98**,559 (1996).
[10] H.-C Ren. Physica C **303**, 115 (1998).
[11] D. N. Basov et al., Phys. Rev. Lett. **77**, 4090 (1997).
[12] R. M. May, Phys. Rev. **115**, 254 (1959).
[13] W. Zhu, H. Kang, Y.C. Lee and Jin-Chang Chen, Phys. Rev. B **50**, 10302 (1994).